*Journal of Sound and Vibration* (1999) **226**(1), 41–55
*Article No.* jsvi.1999.2281, available online at http://www.idealibrary.com on IDEAL®

# FREE VIBRATION OF LONGITUDINALLY STIFFENED CURVED PANELS WITH CUTOUT

B. SIVASUBRAMONIAN,
*Launch Vehicle Design Group, Vikram Sarabhai Space Centre, Thiruvanandapuram*, 695 022.

G. V. RAO
*Structural Engineering Group, Vikram Sarabhai Space Centre, Thiruvanandapuram*, 695 022.

AND

A. KRISHNAN
*Aero Space Engineering Department, Indian Institute of Technology, Madras, Tamil Nadu*, 600 036

(*Received* 18 *November* 1997, *and in Final form* 23 *February* 1999)

Free vibration characteristics of longitudinally stiffened square panels with symmetrical square cutouts are investigated by using the finite-element method. A rectangular shell element with seven degrees of freedom per node together with a beam element of seven degrees of freedom per node is used for the analysis. Studies are carried out on unstiffened as well as stiffened panels keeping the size, weight and boundary conditions the same. Numerical results indicate that the frequency of the stiffened panel is higher. Maximum increase in fundamental frequency is observed on the panel with the smallest radius of curvature.



## 1. INTRODUCTION

Sheet-stiffener combination provides the maximum strength-to-weight ratio for any structure and hence becomes the obvious choice in the construction of aircraft and missile. For inspection as well as for accessing the systems within, cutouts are provided at various locations. For aerodynamic considerations, stiffeners will be provided inside the hull of aircraft; and for space structures the stringers can be provided outside if that is more structurally efficient. Normally, thin-walled open sections like I, Z, Channel, etc. are used as stringers and an optimum structure can be realized by having specific sheet-stiffener construction combinations. To get an exact solution to this practical problem seems difficult, if not impossible, since stiffened panels with cutouts are more involved than those of unstiffened panels due to the change in mass and stiffness distribution.

Analysis of stiffened plates are carried out normally by energy methods by adding energies due to plate and stiffener. Compatibility of displacements at the

0022-460X/99/360041 + 15 $30.00/0 

stiffener and plate have to be ensured. The energy stored in the stiffener will depend on its cross-section and if it is a thin-walled open section, the effect of twisting as well as warping have to be included. Free vibration of a rectangular plate with edge restraints and intermediate stringers have been carried out by Wiu and Lim [1] making use of the Rayleigh–Ritz method. The point of interest in the study has been to quantify the effect of the relative dimensions of the stringer on the frequency of the elastically restrained stiffened plate. Kirk [2] has used the Rayleigh–Ritz method to study the natural frequencies of the simply supported and clamped plates. The dimension of the sheet and stiffener are adjusted to make the weight of the sheet-stiffener combination constant. Chen [3] has made use of the spline component strip method to study the free vibration of stiffened plates. Results are presented for all sides simply supported, three sides clamped and one side simply supported, three sides simply supported and one side clamped conditions. Bhat [4] has studied the effect of spacing of stringers on the natural frequencies of a square plate with simply supported constraints on all four sides. When the stiffener spacing is smaller near the boundary, there is a slight increase in the frequency. The Rayleigh–Ritz method is used for the study. Liu and Chen [5] have used the finite-element method to study the free vibration characteristics of a skew cantilever plate with stiffeners. The influence of the stiffener length, depth and location are studied. Skew plates have increased flexural rigidity compared to rectangular plates and the length of the stiffener does not have a significant effect in increasing the natural frequency. Koko and Olson [6] have used a combination of rectangular cantilever plate elements with 55 degrees of freedom and a beam element with 18 degrees of freedom to determine the static and free vibration behaviour of a stiffened plate. Satisfactory results were found to be feasible with few elements. Rectangular cantilever plates with an $a/L$ ratio of 2 and with different dimensions of stiffeners are analyzed. A plate element developed using the Reissner–Mindlin thick plate theory along with a consistent stiffener element was studied by Holopanien [7]. Clamped plates with stiffeners in one as well as in two directions are analyzed. The finite-element method is also employed to study the behaviour of curved panels. Mustafa and Ali [8] used an eight-noded orthogonally stiffened finite element to study the free vibration of a stiffened cylindrical shell with diaphragm ends. The element is also used to determine the natural frequency of free-free as well as clamped–free curved panels. Palani [9] studied the static and free vibration characteristics of eccentrically stiffened panels (both straight and curved) by two separate isoparametric models QS851 and QL951. Sewall and Naumann [10] have studied the free-vibration performance of longitudinally stiffened shells having closely spaced stiffeners located internally or externally to the shell. Experimental as well as analytical solutions are presented for shells with different boundary conditions. Analytical results were obtained by the energy method employing the Rayleigh–Ritz procedure. In this, longitudinal modes are approximated by a beam vibration function chosen to satisfy the prescribed end conditions and the circumferential modes are expressed by tigonometric functions. Vibration of the simply supported cylindrical shell with the longitudinal stiffener is investigated by Rinehart and Wang [11] using the energy method. Donnell's approximate theory and Flugge's more exact theory are used for the shell while the beam is

characterized by Vlasov's thin-walled beam theory. A sinusoidal wave form for the longitudinal direction and a Fourier series for the circumferential direction are used for the computation of energy. Numerical results are compared with the existing experimental results. A plate with centrally placed stiffener has been studied by Mukherjee and Mukopadyay [12]. An isoparametric stiffened plate element is used in the analysis considering shear deformation so as to analyze thick and thin plates. These results are compared with those of Olson and Hazel [13]. Aksu and Ali [14] studied the stiffened plates by the finite-difference method. Stiffened shells are investigated by Sinha and Mukopadyay [15] using a high-precision triangular shallow shell element in which stiffener orientation can be discrete and not necessarily through the nodal line. Novzhilov's shallow shell theory with a cubic polynomial for transverse displacements and a quintic polynomial for normal displacements are used for the study. Stiffener displacement relations are the same as those of the shell element. The shell element by Olson and Lindberg [16] having seven degrees of freedom per node is reported to yield acceptable results for curved panels with different radii of curvature. The same shell element was successfully used by Sivasubramonian *et al.* [17] to study the effect of curvature and cutouts on square panels with different boundary conditions. The size of the cutout (symmetrically located) as well as curvature of the panels are varied.

The same shell element together with the beam element of Rinehart and Wang [11] are used for the present analysis. Cantilever and clamped panels are studied and from the results it is seen that for panels without cutouts, the maximum effect of stiffening is felt for plate, i.e. when the radius of curvature is very large. Analysis is also carried out on stiffened panels having a cutout with half the size of the side of the plate and the percentage decrease in frequency is felt more for stiffened panels than for the unstiffened.

## 2. FORMULATION

### 2.1. SHELL ELEMENT

Four-noded circular cylindrical rectangular shell elements using the thin-shell theory is developed in line with the formulation given by Olson and Lindberg [16]. The Kirchoff–Love hypothesis is used for the strain–displacement relationships. The higher order terms in the strain energy expression are considered in the present numerical integration. Similarly, the effect of rotary inertia is neglected in the computation of mass matrices for the shell. The element has seven degrees of freedom per node and the nodal variables are $\partial w/\partial x, \partial w/\partial y, w, \partial u/\partial y, u\, \partial v/\partial y, v$. The co-ordinate system is shown in Figure 1. The displacement polynomial for the $w$, $u$ and $v$ displacements are

$$w(x, y) = a_1 + a_2 x + a_3 y + a_4 xy + a_5 x^2 + a_6 y^2 + a_7 x^2 y + a_8 y^2 + a_9 x^3 + a_{10} y^3 + a_{11} x^3 y + a_{12} xy^3,$$

$$u(x, y) = a_{13} + a_{14} x + a_{15} y + a_{16} xy + a_{17} y^2 + a_{18} xy^2 + a_{19} y^3 + a_{20} xy^3,$$

$$v(x, y) = a_{21} + a_{22} x + a_{23} y + a_{24} xy + a_{25} y^2 + a_{26} xy^2 + a_{27} y^3 + a_{28} xy^3.$$

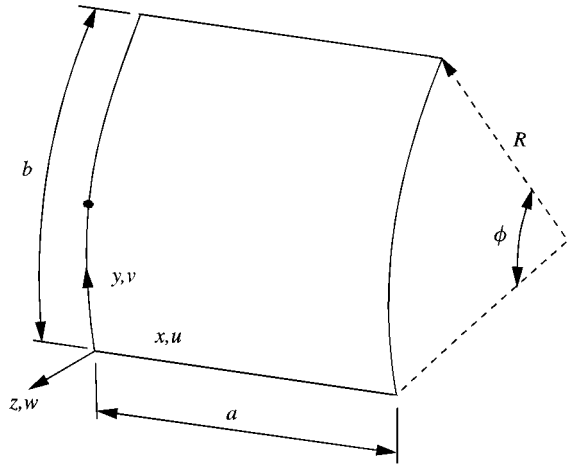


Figure 1. Shell element co-ordinates.

The radial displacement function is the same as that is used in solving quadrilateral plate elements. Since the edges $y = 0$ and $y = b$ are straight, only linear variation in $x$ is used for the inplane displacements, and to include the effect of curvature, higher order terms are used for $y$. The strain–displacement relationships of Love [18] for a classical thin shell is used for the development of the stiffness matrix. They are

$$\varepsilon_x = \partial u/\partial x - z\,\partial^2 w/\partial x^2,$$

$$\varepsilon_y = \partial v/\partial y + w/R - z(\partial^2 w/\partial y^2 - (1/R)\,\partial v/\partial y),$$

$$\varepsilon_{xy} = \partial v/\partial x + \partial u/\partial y - 2z(\partial^2 w/\partial x\,\partial y - (1/\mathrm{R})\,\partial v/\partial x).$$

The strain energy of an isotropic, elastic thin-shell element is given by

$$U_1 = \frac{1}{2}\int_0^b \int_0^a \int_{-h/2}^{h/2} \frac{E}{(1-v^2)}\left[\varepsilon_x^2 + \varepsilon_y^2 + 2v\varepsilon_x\varepsilon_y + \frac{1-v}{2}\,\varepsilon_{xy}\right] \mathrm{d}z\,\mathrm{d}y\,\mathrm{d}x.$$

Closed-form integration is carried out using Castigliano's theorem considering the corner displacements as generalized co-ordinates to obtain the stiffness matrix of the shell element.

The kinetic energy of the cylindrical shell element is given by

$$T_1 = \frac{1}{2}\int_0^b \int_0^a \int_{-h/2}^{h/2} \rho\,[\dot{u}^2 + \dot{v}^2 + \dot{w}^2]\,\mathrm{d}z\,\mathrm{d}x\,\mathrm{d}y.$$

Superscript $(\,.\,)$ denotes differentiation with respect to time. The rotary inertia of the element is considered small and hence neglected. Considering sinusoidal displacements with respect to time and integrating over the thickness of the shell, the

kinetic energy is given by

$$T_1 = \frac{\omega^2}{2} \int_0^b \int_0^a \rho h [u^2 + v^2 + w^2] \, dx \, dy.$$

Here again, the procedure for developing the mass matrix is similar to that for generating the stiffness matrix. In generating the mass matrix the D'Alembert's forces and displacements are related. The stiffness and mass matrices of the cylindrical shell element are symmetric.

## 2.2. STIFFNER ELEMENT

The stiffener element for longitudinal stiffening of a cylindrical shell is a two-noded line element developed from Vlasov's thin-walled beam theory [11]. In this reference, the beam displacements are derived from the shell's mid-surface displacements which in turn are obtained by assuming a Fourier series. In the present formulation, the beam element stiffness matrices are derived using appropriate displacement polynomials. The local co-ordinate system of the beam and shell are matched and the degrees of freedom for the beam are $u$, $v$, $\partial v/\partial x$, $w$, $\partial w/\partial x$, $\theta$, $\partial\theta/\partial x$. There are seven-degrees-of-freedom for each node of which only $u$, $v$ $w$ and $\partial w/\partial x$ are matched with the shell. $\partial v/\partial x$ is essential for transverse bending and $\theta$ and $\partial\theta/\partial x$ are required for twisting and warping. Since the study is on longitudinal stiffening effects, $\partial u/\partial y$ and $\partial v/\partial y$ of the shell are not matched with those of the beam. The displacement polynomials for the beam are

$$u^*(x) = b_1 + b_2 x,$$

$$v^*(x) = b_3 + b_4 x + b_5 x^2 + b_6 x^3,$$

$$w^*(x) = b_7 + b_8 x + b_9 x^2 + b_{10} x^3,$$

$$\theta^*(x) = b_{11} + b_{12} x + b_{13} x^2 + b_{14} x^3.$$

Cubic polynomials are assumed for the longitudinal bending and transverse bending, twisting and warping of the cross-section and linear function for the axial motion. The relevant strain/curvature–displacement relationships for the beam are as given below:

| | |
|---|---|
| Axial | $\varepsilon_x = \partial u^*/\partial x,$ |
| $v$ bending | $\varepsilon_y = \partial^2 v^*/\partial x^2,$ |
| $w$ bending | $\varepsilon_z = \partial^2 w^*/\partial x^2,$ |
| Polar bending | $\varepsilon_{yz} = 2(\partial^2 v^*/\partial x^2)(\partial^2 w^*/\partial x^2),$ |
| Twisting | $\gamma_x = (\partial\theta/\partial x),$ |
| Warping | $\gamma_{xx} = (\partial^2\theta/\partial x^2)$ |

The shell displacements $u$, $v$ and $w$ are related to beam displacements $u^*$, $v^*$, $w^*$ and $\theta$ with respect to the beam shear centre as given below:

$$u^* = u + y_s(\partial v/\partial x) + z_s(\partial w/\partial x),$$

$$v^* = v + z_s\theta,$$

$$w^* = w - y_s\theta.$$

It is assumed that the stiffener is rigidly attached to the shell along a single line and $\theta$ is the angle of twist of the stiffener. The approximation that $\theta$ is equal to $\partial w/\partial y$ of the shell used in reference [11] is followed in the present computation also. $y_s$ and $z_s$ are the distances of the attachment line from the stiffener centroid. The strain energy of the stiffener is given by

$$U_2 = \frac{E^*}{2}\int^l \left[ A\left(\frac{\partial u}{\partial x}\right)^2 + I_{zz}\left(\frac{\partial^2 v}{\partial x^2}\right)^2 + I_{yy}\left(\frac{\partial^2 w}{\partial x^2}\right)^2 + 2I_{yz}\left(\frac{\partial^2 v}{\partial x^2}\right)\left(\frac{\partial^2 w}{\partial x^2}\right) + C_w\left(\frac{\partial^2 \theta}{\partial x^2}\right)^2 + GJ\left(\frac{\partial \theta}{\partial x}\right)^2 \right] \mathrm{d}x$$

$E^*$ is the Young's modulus for the beam material. $A$ is the cross-sectional area of the beam and $I_{yy}, I_{zz}$ and $I_{yz}$ are the second moments of the cross-sectional area about the centroidal axis, $c_w$ is the warping rigidity and $GJ$ is the torsional rigidity.

Beam-shape functions are derived from the assumed polynomial and the strain energy is computed with respect to the transferred displacements from the shell mid surface. A stiffness matrix for the beam element is derived by integrating the strain energy expression as carried out for the shell.

The kinetic energy of the stiffener is given by

$$T_2 = \frac{\rho}{2}\int \left[ u^{*^2} + v^{*^2} + w^{*^2} - 2y_c\theta + 2z_c\theta + I_p\theta^2 + I_{yy}\left(\frac{\partial \dot{w}}{\partial x}\right)^2 + I_{zz}\left(\frac{\partial \dot{v}}{\partial x}\right)^2 - I_{yz}\left(\frac{\partial \dot{v}}{\partial x}\,\frac{\partial \dot{w}}{\partial x}\right) \right] \mathrm{d}x.$$

$\rho^*$ is the mass density of the stiffener, $I_p$ is the polar moment of inertia, $yc$ and $zc$ are the distances of the centroid with respect to the shear centre of the cross-section. Integration of the strain energy and kinetic energy gives the beam stiffness and mass matrices. Stiffness matrix $[K_s]$ of the shell elements, stiffness matrix $[K_b]$ of the stiffener element, mass matrix $[M_s]$ of the shell element and mass matrix $[M_b]$ of the stiffener are thus obtained. In the assembly, stiffness and mass matrices of the shell and the stiffener are assembled using the standard finite-element procedure:

$$[K] = [K_s] + [K_b], \qquad [M] = [M_s] + [M_b],$$

where $[K]$ and $[M]$ are the assembled stiffness and mass matrices. The eigenvalue problem is given by

$$[[k] - \lambda[M]]\{q\} = 0.$$

The solution algorithm by Corr and Jennings [19] is used to obtain the frequencies and mode shapes for the various modes.

## 3. NUMERICAL RESULTS AND DISCUSSIONS

A simply supported shell stiffened using four equally spaced stiffeners defined in reference [11] has been analyzed to validate the code. A half-shell model (circumferentially half) with a $20 \times 20$ mesh and symmetric boundary conditions is studied. Stiffener and shell properties are defined in Table 1. The present results are compared modewise with the computation made using the Flügge theory and experimentally obtained frequencies reported in reference [11]. These comparisons are given in Table 1. The present computation shows a marginal increase in frequency with respect to the Flügge theory and experimental results. The assumption of zero shell rotary inertia and the linear transformation of shell displacement into those of the stiffener might have led to a stiffer shell in comparison to the Flügge's theory (Figure 2). Experimental results from reference [11] vary within 6% for the first few modes and the fundamental frequency agrees well. The higher magnitude of the finite-element results *vis-à-vis* the experimental values may be due to the boundary condition effect.

An all side clamped and centrally stiffened square plate having a thickness of 1·37 mm was analyzed and compared with references [12–13]. A stiffener of 6·35 mm width and 12·7 mm height is centrally placed in the plate. Results given in Table 2 agree well with the theoretical values of reference [13], while the experimental values are lower. The lower value can be due to the assumption of fully clamped boundary condition in the finite-element analysis as explained earlier. Computation carried out by Mukherjee and Mukopadyay [12] is on the higher side except for the fundamental mode. However, this study indicates that the percentage difference between the present formulation and the other two theories are within 5%.

### 3.1. EFFECT OF STIFFENING

After completing the validation, studies are carried out on curved cantilever panels/plates (C–F–F–F) and curved clamped panels/plates (C–C–C–C). For both panels, three stiffeners (I sections) are used as shown in Figures 3 and 4. For C–F–F–F panels, the stiffeners are at the centre and the two circumferential edges whereas for the C–C–C–C panels, they are at $b/4$, $b/2$ and $3b/4$.

In the present study, the ratio of the area of the stiffener to that of the shell is to be taken as 3 : 7. This ratio is a viable configuration for a practical problem. Results are presented in Table 3 together with the material properties and the geometric details

TABLE 1

*Simply supported longitudinally stiffened shell. Shell geometry*: $R = 7{\cdot}657''$, $h = 1{\cdot}826$ e-02″, $l = 38{\cdot}8''$, $E = 24{\cdot}8$e 06 psi, $\mu = 0{\cdot}3$, $\rho = 6{\cdot}95$e-04 lbs$^2$/in$^4$; *Stiffener geometry*: $A = 1{\cdot}589$e-02″, $I_{zz} = 1{\cdot}493$e-04 in, $I_{yy} = 3{\cdot}38$e-04 in, $zs = -0{\cdot}208''$, $zc = 0{\cdot}372''$, $yc = 0{\cdot}372''$, $cw = 2{\cdot}96$e-06 in$^6$, $E = 30{\cdot}0$e 06psi, $\mu = 0{\cdot}3$, $\rho = 6{\cdot}95$e-04 lbs$^2$/in$^4$

| Mode $m$, $n$ | Frequency (Hz) Present | Flugge's theory | Experimental [11] |
|---|---|---|---|
| 1,5 | 92·5 | 92 | 89 |
| 1,4 | 106·5 | 105 | 100 |
| 1,6 | 107·7 | 108 | 104 |
| 1,7 | 147·7 | 140 | 137 |
| 1,3 | 159·8 | 164 | 156 |
| 1,8 | 177·9 | 173 | 174 |
| 1,9 | 231·8 | 228 | 224 |

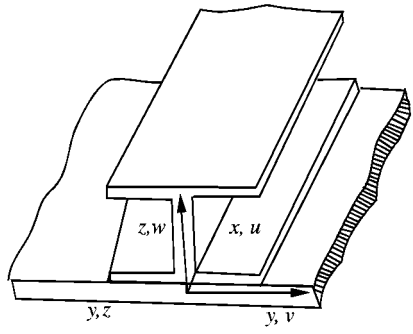


Figure 2. Stiffener element co-ordinates.

TABLE 2

*Frequencies for an all sided clamped plate with central stiffener. Size of the plate* = 203 mm × 203 mm × 1·37 mm *thickness, Size of the stiffener* = 6·35 mm × 12·7 mm, $E = 7020$ kg/mm$^2$, $\rho = 2{\cdot}72$ e-10 kg-s$^2$/mm$^4$, $\mu = 0{\cdot}3$

| Mode | Present 16 × 16 mesh | Olson and Hazel [13] Theory | Experimental [14] | Mukherjee and Mukhopadyay |
|---|---|---|---|---|
| 1 | 729·6 | 718·1 | 689 | 711·8 |
| 2 | 748·0 | 751·4 | 725 | 768·2 |
| 3 | 1009·1 | 997·4 | 961 | 1016·5 |
| 4 | 1016·6 | 1007·1 | 986 | 1031·9 |
| 5 | 1321·8 | 1419·8 | 1376 | 1465·2 |

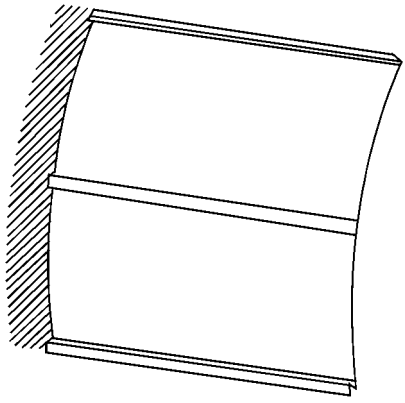

Figure 3. Stiffener cantilever panel.

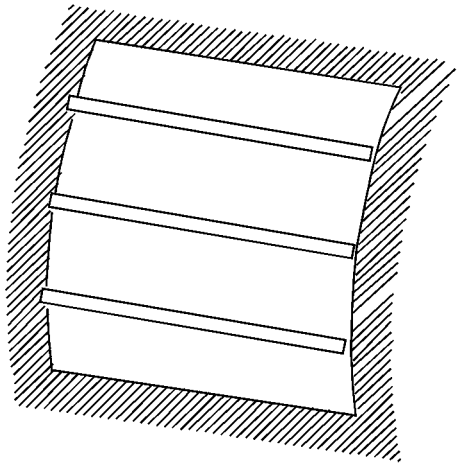

Figure 4. Stiffened clamped panel.

of the sheet as well as the stiffener. Four values of radius ( $\infty$ , 2000 mm, 500 mm and 200 mm) are chosen for the study and the first five frequencies together with the associated mode shapes are given in the table. The value of radius $R$ is kept constant in the computation which means that $R/h$ for unstiffened and stiffened panels will be different. In the table, configuration A corresponds to the unstiffened panel and configuration B corresponds to the stiffened one. It can be seen that for all panels studied, there is an increase in all frequency values for the corresponding modes due to stiffening. The percentage increase in the frequency depends on the mode and for higher modes the increase in the value is less than that for the fundamental mode for all panels. Increase in frequency for particular mode is maximum for the plate (panel with maximum radius) and with a decrease in radius, the relative magnitude of frequency due to stiffening reduces. This could be attributed to the predominance of bending of panels with larger radii when the stiffener effect is dominant. There is a change in mode shape also with the

TABLE 3

*Effect of curvature on* C–F–F–F *and* C–C–C–C *panels. Configuration* A = *Unstiffened panel, Configuration* B = *Panel stiffened with three stiffeners, Panel geometry*: $R = 500$ mm, 500 mm × 500 mm × 2 mm *for configuration A*, 500 mm × 500 mm × 1·4 mm *for configuration B, Stiffener geometry*: $A = 100$ mm$^2$, $I_{yy} = 8603$ mm$^4$, $I_{zz} = 1138$ mm$^4$, $J = 1138$ mm$^4$, $zc = 12{\cdot}5$ mm, $cw = 1{\cdot}62\text{e}05$ mm$^6$

| | | C–F–F–F | | | | C–C–C–C | | | |
|---|---|---|---|---|---|---|---|---|---|
| | Mode | Config. A | | Config. B | | Config. A | | Config. B | |
| $R$ | No. | Freq. | $m,n$ | Freq. | $m,n$ | Freq. | $m,n$ | Freq. | $m,n$ |
| Plate | 1 | 6·8 | 1,1 | 67·3 | 1,1 | 69·2 | 1,1 | 350·8 | 1,4 |
| | 2 | 16·5 | 1,2 | 68·4 | 1,2 | 140·9 | 1,2 | 382·5 | 1,3 |
| | 3 | 41·1 | 2,1 | 115·9 | 1,3 | 140·9 | 2,2 | 426·2 | 1,2 |
| | 4 | 52·4 | 1,3 | 121·5 | 1,2 | 206·9 | 3,2 | 428·9 | 1,1 |
| | 5 | 59·7 | 2,2 | 130·9 | 2,1 | 252·6 | 3,1 | 461·6 | 1,6 |
| 2000 | 1 | 22·8 | 1,2 | 68·1 | 1,2 | 213·9 | 1,2 | 356·9 | 1,4 |
| | 2 | 37·4 | 1,1 | 74·3 | 1,1 | 243·2 | 1,3 | 401·3 | 1,3 |
| | 3 | 65·6 | 1,3 | 131·3 | 1,4 | 326·1 | 2,4 | 464·6 | 1,2 |
| | 4 | 90·3 | 2,2 | 134·2 | 1,3 | 333·3 | 2,3 | 474·4 | 1,4 |
| | 5 | 96·5 | 2,3 | 166·5 | 2,4 | 393·7 | 1,1 | 507·8 | 2,4 |
| 500 | 1 | 52·2 | 1,3 | 82·0 | 1,2 | 404·7 | 1,3 | 412·9 | 1,4 |
| | 2 | 55·5 | 1,2 | 87·1 | 1,3 | 413·4 | 1,4 | 525·3 | 1,3 |
| | 3 | 138·5 | 1,4 | 156·5 | 1,4 | 614·3 | 1,5 | 640·4 | 1,4 |
| | 4 | 156·6 | 2,3 | 183·2 | 1,5 | 617·2 | 2,4 | 765·3 | 1,5 |
| | 5 | 159·7 | 2,4 | 265·8 | 1,6 | 638·2 | 2,5 | 772·7 | 1,6 |
| 200 | 1 | 79·0 | 1,3 | 93·0 | 1,3 | 609·9 | 1,4 | 602·8 | 1,4 |
| | 2 | 88·6 | 1,4 | 95·0 | 1,4 | 612·9 | 1,5 | 763·8 | 1,5 |
| | 3 | 211·2 | 1,4 | 215·2 | 1,5 | 839·5 | 1,6 | 864·9 | 1,6 |
| | 4 | 227·7 | 1,5 | 250·6 | 1,4 | 885·7 | 1,5 | 905·1 | 1,5 |
| | 5 | 234·2 | 2,3 | 279·3 | 1,6 | 963·7 | 2,5 | 1014·3 | 1,8 |

introduction of the stiffener and this could be due to the predominance of modes on bending or twisting. Another feature noticed is that there are different frequencies for the same mode shapes. This could be due to the difference in the rigidity of the panel in the radially inward and outward directions. To substantiate this, a plot is given in Figure 7 for the C–F–F–F plate for which the second and fourth mode shapes are the same. Since $m = 1$ for both, the plot is presented only for $n$ (circumferential mode). Though the number of modes is the same, the pattern is different causing a change in frequencies.

The behaviour is different for C–C–C–C panels. For plate and $R = 2000$ mm, the effect of stiffening is one of increasing the overall frequencies, but for $R = 500$ mm and 200 mm such behaviour is not seen. The mode shape for the corresponding frequency differs for the unstiffened and stiffened panels. Here again, there are two

frequencies for the same mode shape and for $R = 200$ mm, the second and fourth mode shapes are the same and correspond to (1, 5).

### 3.2. EFFECT OF CUTOUT ON STIFFENING

Results for the C–F–F–F and C–C–C–C panels with cutouts are presented in Table 4. 25% of the area of the panel is removed from the centre ($g = a/2$) where $g$ refers to the side of the square cutout. The effect of cutout is (Figures 5–7) to reduce the frequency for all C–F–F–F panels. The maximum reduction is felt on the fundamental frequency of the stiffened plate (value reduces from 56·8 Hz to 18 Hz). There is an interchange of mode shapes due to cutouts for all C–F–F–F panels

TABLE 4

*Effect of cutout* (250 × 250 mm) C–F–F–F *and* C–C–C–C *panels. Configuration A = Unstiffened panel, Configuration B = Panel stiffened with three stiffeners, Panel geometry*: $R = 500$ mm, 500 mm × 500 mm × 2 mm *for configuration A*, 500 mm × 500 mm × 1·4 mm *for configuration B*, *Stiffener geometry*: $A = 100$ mm$^2$, $I_{yy} = 8603$ mm$^4$, $I_{zz} = 1138$ mm$^4$, $J = 1138$ mm$^4$, $zc = 12{\cdot}5$ mm, $cw = 1{\cdot}62\text{e}05$ mm$^6$

| | | C–F–F–F | | | | C–C–C–C | | | |
|---|---|---|---|---|---|---|---|---|---|
| | Mode | Config. A | | Config. B | | Config. A | | Config. B | |
| $R$ | No. | Freq. | $m, n$ | Freq. | $m, n$ | Freq. | $m, n$ | Freq. | $m, n$ |
| Plate | 1 | 4·8 | 1,1 | 23·5 | 1,1 | 125·7 | 1,1 | 411·4 | 1,4 |
| | 2 | 9·6 | 1,2 | 57·7 | 1,2 | 147·3 | 2,2 | 411·9 | 1,3 |
| | 3 | 26·3 | 2,1 | 72·3 | 2,3 | 147·3 | 2,1 | 476·6 | 1,2 |
| | 4 | 36·7 | 2,3 | 90·2 | 2,1 | 199·2 | 2,2 | 477·4 | 1,4 |
| | 5 | 38·6 | 1,2 | 106·6 | 1,2 | 205·0 | 3,1 | 487·9 | 2,3 |
| 2000 | 1 | 12·3 | 1,2 | 43·2 | 1,1 | 185·3 | 1,2 | 420·5 | 1,4 |
| | 2 | 23·1 | 1,1 | 56·9 | 1,2 | 188·2 | 1,1 | 421·9 | 1,3 |
| | 3 | 44·6 | 1,3 | 87·9 | 1,3 | 295·9 | 2,1 | 489·9 | 2,4 |
| | 4 | 58·8 | 2,2 | 118·1 | 1,4 | 309·7 | 2,1 | 498·8 | 1,4 |
| | 5 | 61·9 | 2,1 | 124·2 | 2,4 | 345·3 | 3,1 | 509·8 | 2,3 |
| 500 | 1 | 28·1 | 1,2 | 57·6 | 1,2 | 294·0 | 1,4 | 525·5 | 1,4 |
| | 2 | 42·9 | 2,1 | 80·7 | 1,3 | 295·4 | 1,3 | 544·9 | 1,3 |
| | 3 | 105·5 | 1,4 | 114·1 | 1,4 | 537·8 | 2,4 | 652·0 | 2,4 |
| | 4 | 115·9 | 1,1 | 117·1 | 1,5 | 543·4 | 2,3 | 734·9 | 1,4 |
| | 5 | 144·1 | 1,2 | 154·6 | 2,3 | 626·3 | 1,4 | 761·5 | 2,5 |
| 200 | 1 | 43·7 | 2,3 | 60·9 | 1,2 | 433·1 | 1,4 | 759·8 | 1,4 |
| | 2 | 44·5 | 1,2 | 77·9 | 1,3 | 433·7 | 1,3 | 779·4 | 1,5 |
| | 3 | 73·3 | 1,4 | 104·2 | 1,4 | 777·3 | 2,4 | 994·2 | 1,4 |
| | 4 | 134·2 | 1,3 | 131·1 | 1,5 | 789·2 | 2,3 | 1002·0 | 1,5 |
| | 5 | 163·2 | 2,4 | 203·2 | 2,3 | 856·8 | 1,3 | 1081·0 | 2,6 |

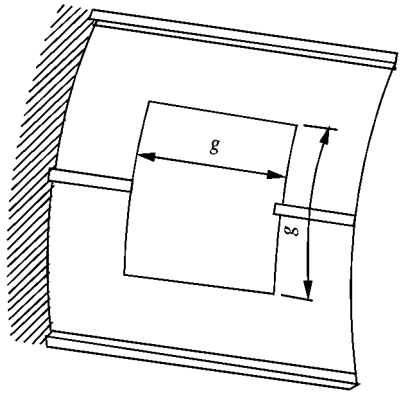


Figure 5. Stiffened cantilever panel with cutout.

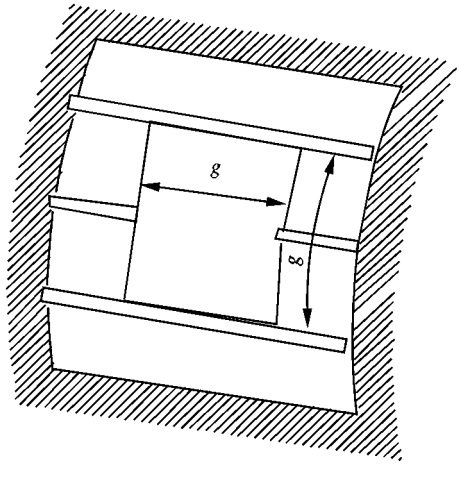


Figure 6. Stiffened clamped panel with cutout.

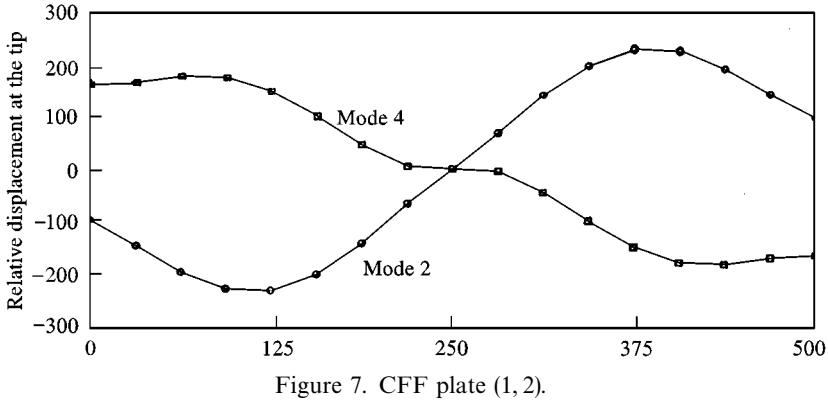


Figure 7. CFF plate (1, 2).

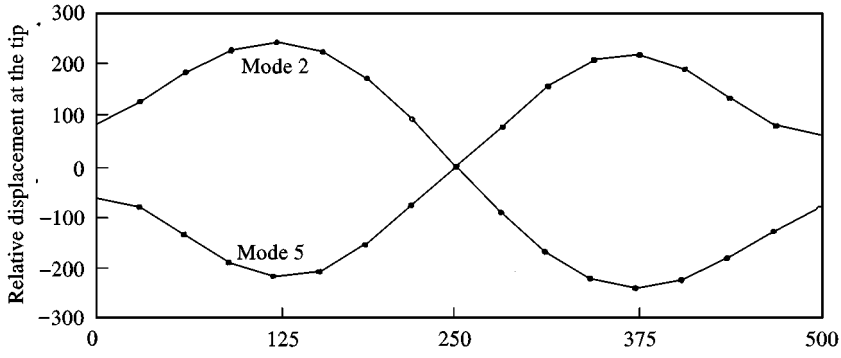


Figure 8. CFF plate with cutout (1, 2).

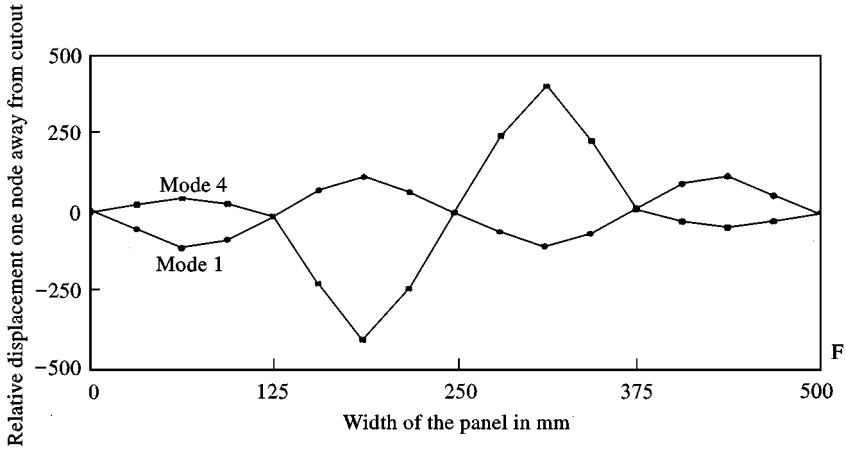


Figure 9. $R = 500$ mm CCCC panel with cutout (1, 4).

studied and mode shapes for curved panels with cutouts do not repeat. However, when a stiffener is used, there are repeated mode shapes and Figure 8 represents the mode shapes 2 and 5 of the stiffened C–F–F–F plate. The trend is different for the C–C–C–C plate and the effect of the cutout is to increase the frequency in almost all the cases. When the edges are clamped, it is seen that the same mode shapes exist with different frequencies for all panels with cutouts. Typically, Figure 9 is presented to identify the mode shapes 1 and 4 for the C–C–C–C stiffened panel with cutout for $R = 500$ mm.

### 3.3. CONCLUSION

Analysis carried out on unstiffened and stiffened cantilever and all side clamped panels keeping the size and weight of the panels constant brings out the following. The ratio of increase in fundamental frequency of the cantilever stiffened plate to that of the unstiffened plate is 8·9 and for stiffened panels this ratio is 0·18 for the

stiffened panel with $R = 200$ mm. For plate/panel clamped on all edges, corresponding values work out as 4·9 and 0·15; these values are 2·27 and 0.75, respectively, when there is cutout. Numerical value indicates that the effect of stiffener is felt more for cantilever panels than clamped panels. The corresponding values of the plate with cutout is 2·28 and for the panel 0·75. Stiffening increases the frequency and the cutout decreases the frequency for all cantilever panels. There is no definite trend found in the case of all side clamped panels for all ranges of curvature. When the radius is large, the effect of the stiffener is to increase the frequency and also that of the cutout. This could be due to an increase in bending stiffness since stiffeners provide bending rigidity and a cutout being at the centre does not cause a large reduction in bending stiffness.

## ACKNOWLEDGEMENTS

We thank the reviewers for their constructive criticism and valuable suggestions.

## REFERENCES

1. J. R. Wiu and W. H. Lim 1988 *Journal of Sound and Vibration* **123**, 103–113. Vibration of rectangular plates with edge restraints and intermediate supports.
2. C. L. Kirk 1970 *Journal of Sound and Vibration* **13**, 375–388. Natural frequencies of stiffened plates.
3. C. S. Chen, W. Liu and S. M. Chern 1994 *Computers and Structures* **50**, 471–480. Vibration analysis of stiffened plate.
4. R. B. Bhat 1982 *Journal of Sound and Vibration* **84**, 449–452. Vibration of panels with nonuniformly spaced stringer.
5. W. H. Liu and W. H. Chen 1988 *Journal of Sound and Vibration* **127**, 384–390. Free vibrations of restrained cylindrical thin shell panel under axial and transverse stresses.
6. T. S. Koko and M. D. Olson 1992 *Journal of Sound and Vibration* **158**, 149–167. Vibration analysis of stiffened plates by super elements.
7. T. P. Holopanien 1995 *Computers and Structures* **56**, 93–1007. Finite element free vibration analysis of eccentrically stiffened plates.
8. B. A. Mustafa and R. Ali 1987 *Journal of Sound and Vibration* **113**, 317–327. Prediction of natural frequency of vibration of stiffened cylindrical shells.
9. G. S. Palani, N. R. Iyer and T. V. R. Appa Rao 1992 *Computers and Structures* **43**, 651–661. An efficient finite element model for static and vibration analysis of eccentrically stiffened plates/shells.
10. J. L. Sewall and E. C. Naumann 1968 *NASA-TND*-4705. An experimental and analytical vibration study in thin cylindrical shells with and without longitudinal stiffeners.
11. S. A. Rinehart and J. T. S. Wang 1972 *Journal of Sound and Vibration* **24**, 151–163. Vibration of simply supported cylindrical shells with longitudinal stiffeners.
12. A. Mukherjee and M. Mukopadyay 1988 *Computers and Structures* **30**, 1303–1317. Finite element free vibration of eccentricity stiffened plates.
13. M. D. Olson and C. R. Hazel 1977 *Journal of Sound and Vibration* **50**, 43–61. Vibration studies on some integral rib stiffened plates.
14. G. Aksu and R. Ali 1976 *Journal of Sound and Vibration* 44,147–158. Free vibration analysis of stiffened plates using finite element method.
15. G. Sinha and M. Mukopadyay 1994 *Journal of Sound and Vibration* **171**, 527–549. Finite element free vibration analysis of stiffened shells.

16. M. D. Olson and G. M. Lindberg *NRC-NAE-LR*-497. A finite cylindrical shell element and the vibrations of a curved fan blade.
17. B. Sivasubramonian, A. M. Kulkarni, G. Venkateswara Rao and A. Krishnan 1997 *Journal of Sound and Vibration* **200**, 227–234. Free vibrations of curved panels with cutouts.
18. A. E. H. Love 1927 *A treatise on Mathematical Theory of Elasticity*, Cambridge: Cambridge University Press, fourth edition.
19. R. B. Corr and A. Jennings 1976 *International Journal of Numerical Methods in Engineering*. **10**, 647–663. A simultaneous iteration algorithm for symmetric eigen value.

## APPENDIX: NOMENCLATURE

| | |
|---|---|
| $E$ | Young's Modulus for shell element |
| $E^*$ | Young's modulus for the beam element |
| $K$ | stiffness matrix |
| $M$ | mass matrix |
| $R$ | panel radius |
| $T$ | kinetic energy |
| $U$ | strain energy |
| $a$ & $b$ | length and width of the element |
| $a_1$–$a_{28}$ | constants of the displacement polynomial for the shell |
| $b_1$–$b_{14}$ | constants of the displacement polynomial for the beam |
| $g$ | side of the square cutout |
| $h$ | shell thickness |
| $m$ | number of half-waves in longitudinal direction |
| $n$ | number of half-waves in circumferential direction |
| $t$ | time |
| $q$ | eigenvector |
| $u, v, w$ | shell displacements in $x$, $y$ and $z$ direction |
| $u^*, v^*, w^*, \theta^*$ | beam displacements axial, bending in two planes and twisting |
| $y_s, z_s$ | distance between the centroid of stiffener and the line of attachment at the shell |
| $y_c, c, z_c$ | distance between the centroid of the stiffener and its shear centre |
| $\phi$ | panel included angle |
| $\lambda$ | eigenvalue |
| $v$ | poisson's ratio |
| $\rho$ | mass density |
| $\omega$ | circular frequency |